Appendix Information

Platinum-induced upregulation of ITGA6 promotes chemoresistance and spreading in ovarian cancer

Alice Gambelli, Anna Nespolo, Gian Luca Rampioni Vinciguerra, Eliana Pivetta, Ilenia Pellarin, Milena S. Nicoloso, Chiara Scapin, Linda Stefanatti, Ilenia Segatto, Andrea Favero, Sara D'Andrea, Maria Teresa Mucignat, Michele Bartoletti, Emilio Lucia, Monica Schiappacassi, Paola Spessotto, Vincenzo Canzonieri, Giorgio Giorda, Fabio Puglisi, Andrea Vecchione, Barbara Belletti, Maura Sonego and Gustavo Baldassarre

[1]

Table of Contents

[1]

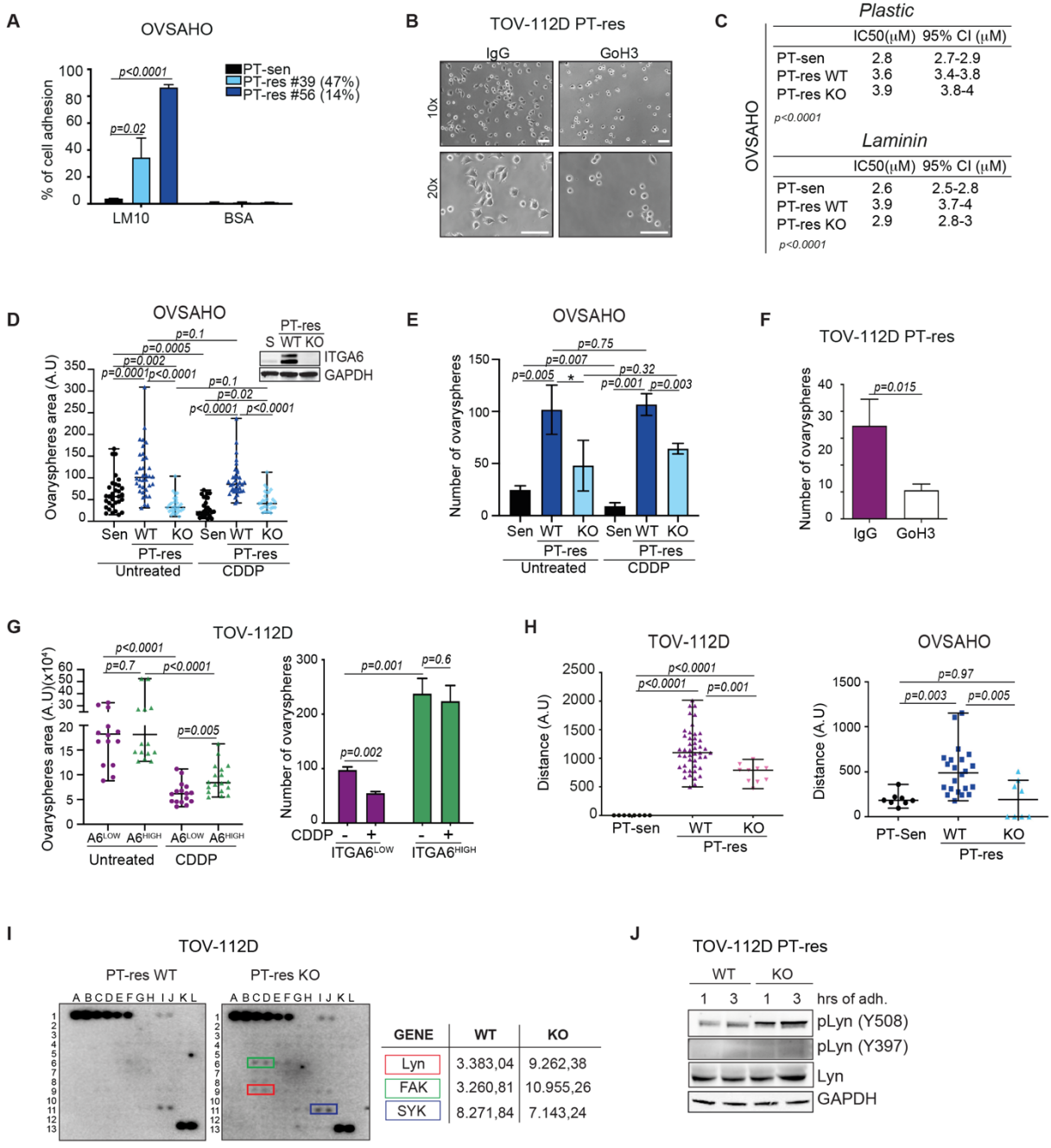

Appendix Figure S1 (related to Figure 3). ITGA6 mediates higher metastatic capability of EOC PT-res cells.

A) Expression of Graph reporting the percentage of cell adhesion on laminin 10 (LM10) coating of OVSAHO PT-sen and PT-res clones measured by CAFCA assay. In the legend is reported the percentage of ITGA6 positive cells for each PT-res clone. B) Representative phase-contrast images, taken with 10X or 20X objectives as indicated, of TOV-112D PT-res cells plated on LM10 coated dishes in the presence of IgG (as control) or of the specific anti-ITGA6 blocking antibody (GoH3 Ab). Scale bars, 50 μm. C) Tables reporting the IC50 and the confidence interval (CI) of OVSAHO

PT-sen, PT-res WT and PT-res ITGA6KO cells plated on plastic or in Laminin and treated with increasing doses of CDDP for 72 hours. Fisher's exact test was used to calculate the global p value reported under the tables. D-E) Graph reporting the area (D) and the number (C) of ovaryspheres formed by OVSAHO PT-sen, PT-res ITGA6WT and ITGA6KO cells treated or not with CDDP (2μM) for 24 hours. Data reported are the mean (±SD) of two independent experiments performed in triplicate, in which at least 10 randomly selected fields were analyzed. The inset in D reports the ITGA6 expression in the used cells analyzed by western blot (S=PT-sen cells). F) Graph reporting the number of ovaryspheres formed by TOV-112D PT-res in presence of IgG (as control) or of GoH3 Ab. G) Graph reporting the area (left) and the number (right) of ovaryspheres formed by TOV-112D ITGA6^{HIGH} and ITGA6^{LOW} subpopulations treated or not with CDDP. Data represent the mean (±SD) of two independent experiments performed in triplicate, in which at least 10 randomly selected fields were analyzed. H) Graph reporting the distance covered by the individual cells from the edge of the drop (mean ± SD of three independent experiments, in which at least 10 randomly selected fields were analyzed) in matrigel evasion assay of TOV-112D (left) and OVSAHO (right) parental, PT-res WT and KO cells. I) Western blots analysis of RTK array using whole cell lysates extracted from TOV112D PT-res ITGA6WT and KO allowed to adhere 3 hrs on LM10 coated dishes. Colored boxed spots highlight differentially expressed RTKs. On the right, the table reports the expression of the three differentially phosphorylated proteins in WT and KO cells, expressed as normalized arbitrary units. J) Western blot analysis evaluating the expression of the indicated proteins in lysates of TOV-112D PT-res ITGA6WT and ITGA6KO cells plated on LM10 coated dishes for 1 and 3 hours. In D and J, GAPDH was used as loading control. In A and D-H statistical significance was determined by a two-tailed, unpaired Student's t-test (Exact *p* values were reported on graphs).

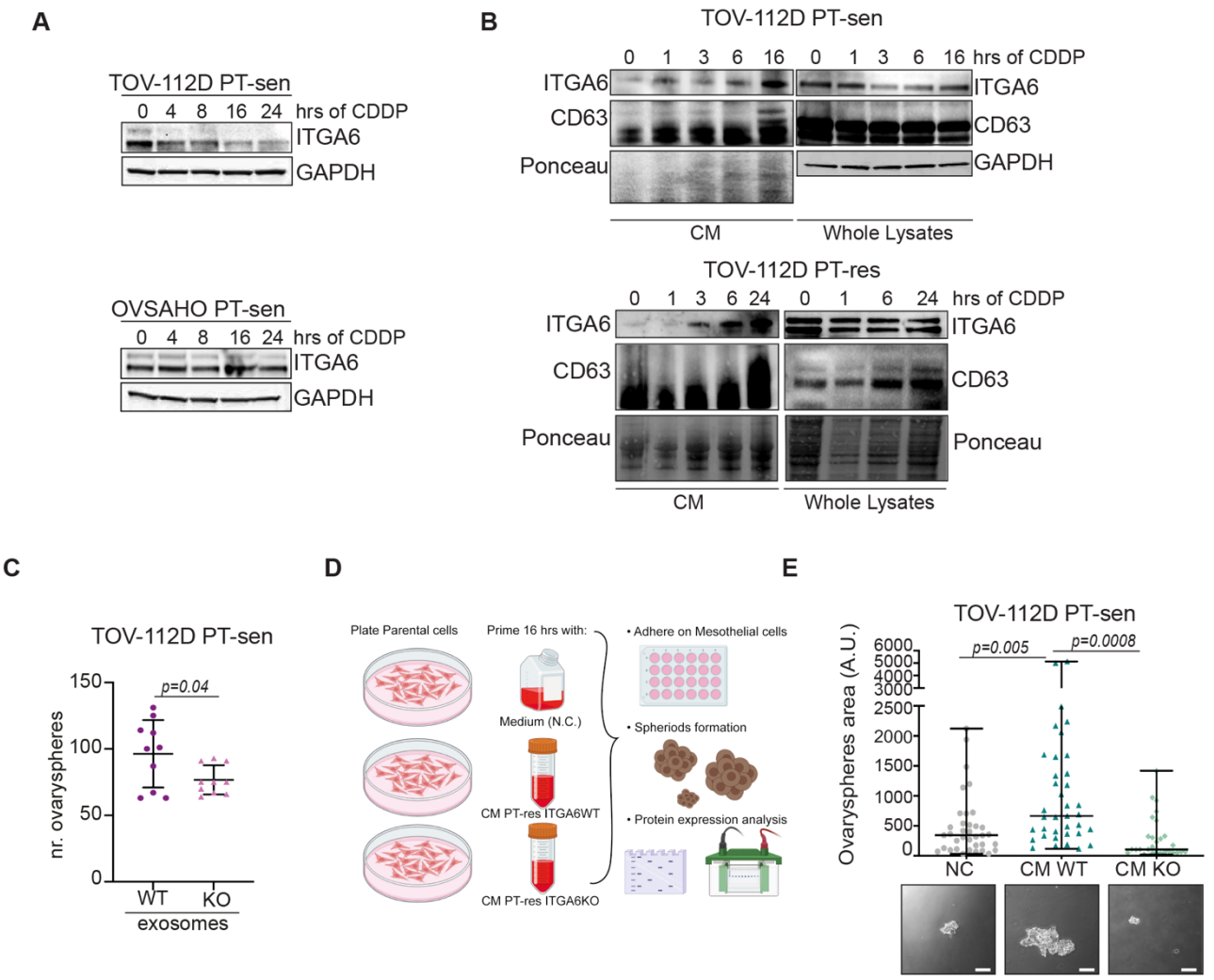

Appendix Figure S2 (related to Figure 4). Secreted ITGA6 primes PT-sen cells to adhere and grow on mesothelial cells

A) Western blot analysis of ITGA6 expression in whole lysates of TOV-112D and OVSAHO PT-sen cells treated with CDDP for the indicated time points. B) Western blot analysis of ITGA6 and CD63 expression in conditioned medium (CM) and whole lysates of TOV-112D PT-sen (top) and PT-res (bottom) cells treated with CDDP (25μM) for the indicated time points. In A and B, GAPDH and Ponceau were used as loading control. C) Graphs reporting the number of ovaryspheres formed by TOV-112D parental cells primed with exosomes of TOV-112D PT-res ITGA6WT and KO cells and then plated on a mesothelial cells monolayer. D) Schematic representation of the experimental procedures utilized to test the biological activity of ITGA6 secreted in contitioned medium (CM). TOV-112D PT-sen cells were incubated for 16 hours with the CM from WT or ITGA6KO TOV-112D PT-res cells or control medium and then challenged in adhesion assays on mesothelial cells, ovaryspheres formation assays or processed for western blot analyses. E) Graph (top) and representative phase-contrast images (bottom) reporting the area of ovaryspheres formed by TOV-112D parental cells treated as specified in D then plated on polyhema-coated dishes. Scale bar =

50μM In C and E, statistical significance was determined by a two-tailed, unpaired Student's t-test (Exact *p* values were reported on graphs).

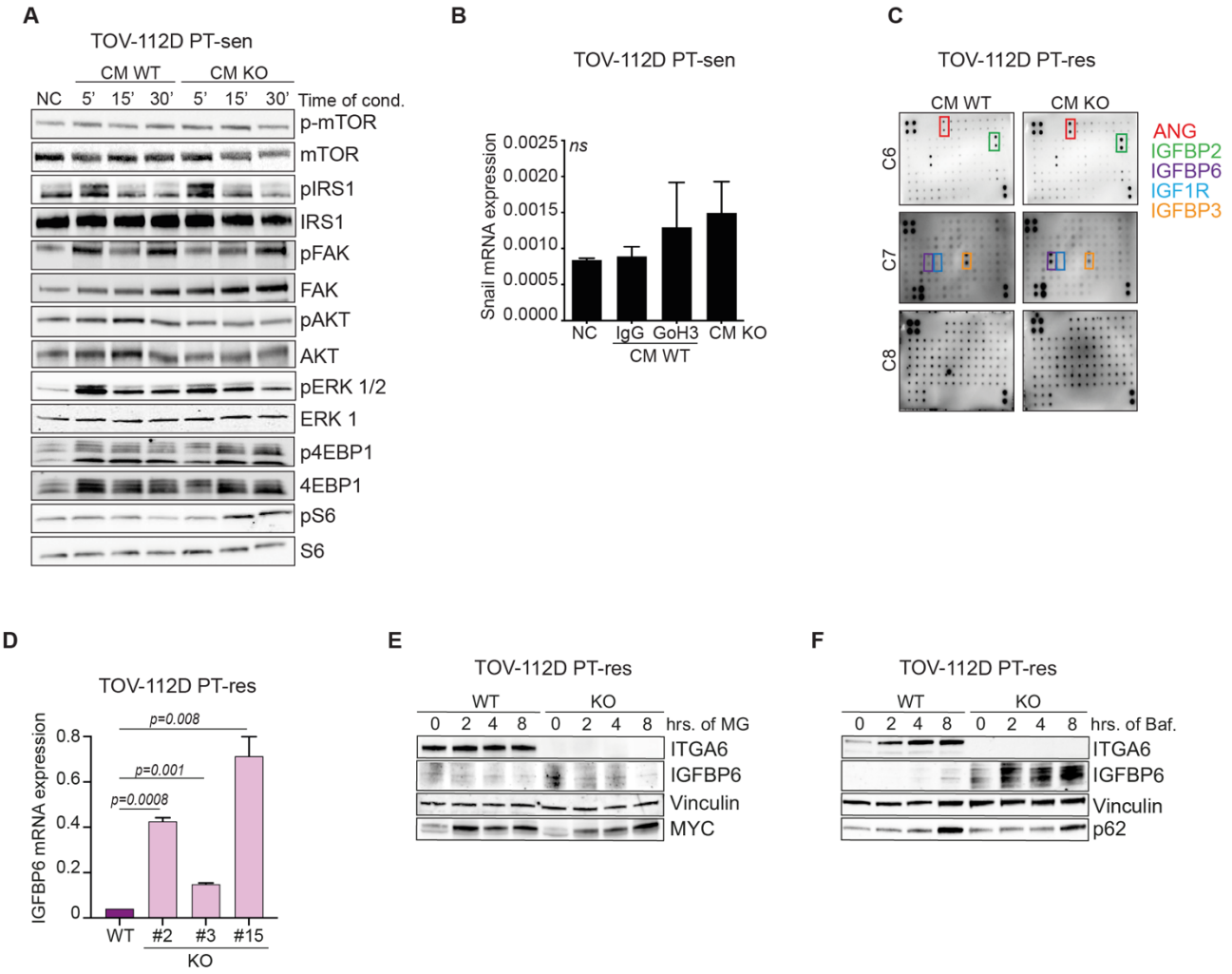

Appendix Figure S3 (related to Figure 4).

A) Western blot analysis of the indicated proteins in whole lysates of TOV-112D PT-sen cells challenged or not for the indicated time points with CM of TOV-112D PT-res WT or ITGA6KO cells. B) Graph reporting the mRNA expression of Snail in TOV-112D PT-sen cells challenged with CM of PT-res ITGA6 WT in presence or not of the specific anti-ITGA6 GoH3, or with CM of PT-res ITGA6 KO cells. C) Western blots of cytokine arrays (C6-C8 arrays) using CM of TOV112D PT-res WT and ITGA6KO cells. The most significantly differentially expressed proteins are highlighted in colored boxes. D) qRT-PCR evaluating the mRNA expression of IGFBP6 in TOV-112D PT-res WT and ITGA6KO clones. Statistical significance was determined by a two-tailed, unpaired Student's t-test (Exact *p* values were reported on graphs). E-F) Western Blot analysis of IGFBP6

expression in TOV-112D PT-res exposed to a time-course treatment with the proteasome inhibitor, MG132 (E) or with inhibitor of autophagosome-lysosome fusion, Bafylomicin (F). MYC and p62 were used as positive control of MG132 and Bafylomicin activity, respectively. Vinculin was used as loading control.

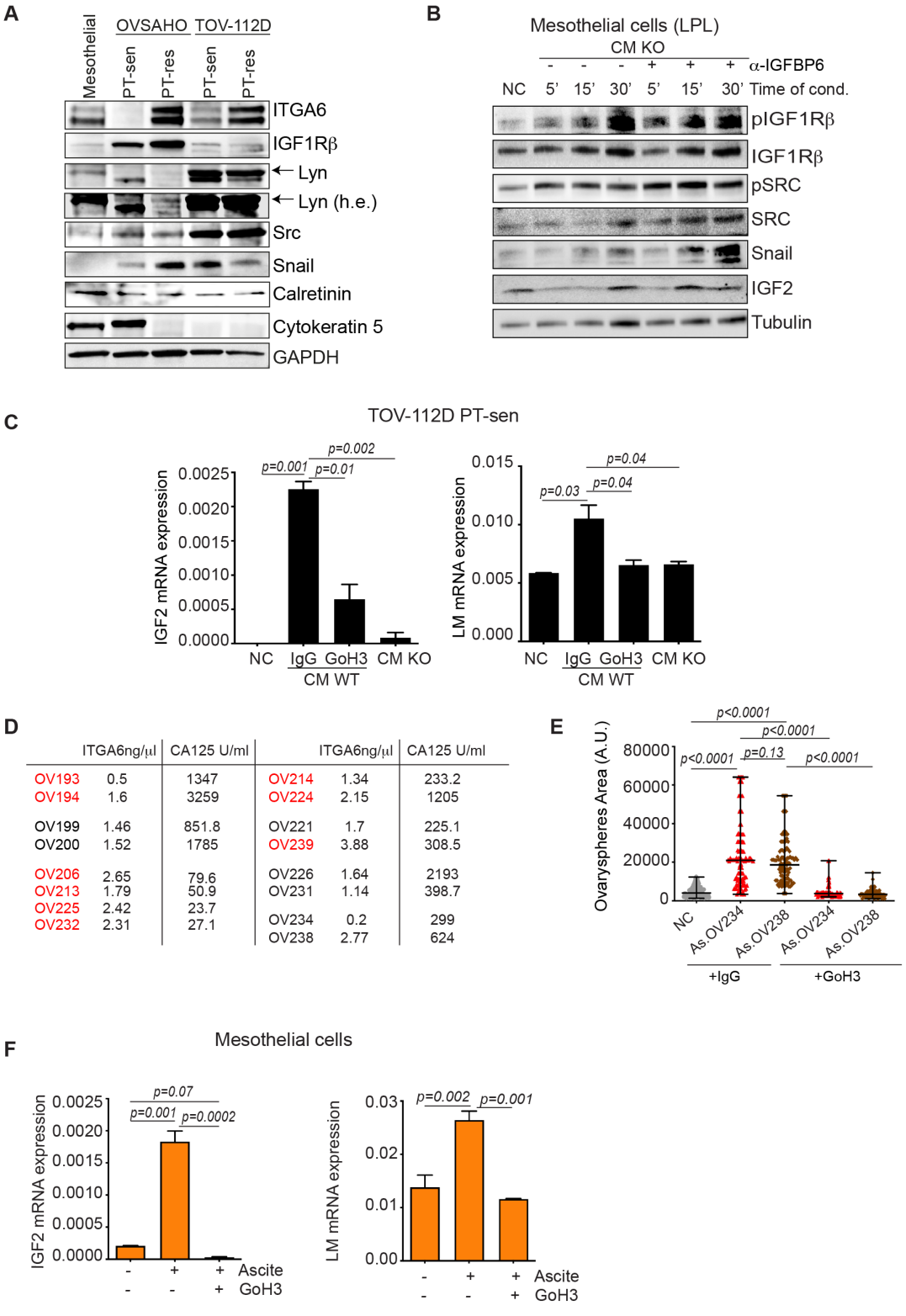

Appendix Figure S4 (related to Figure 5) Secreted ITGA6 primes mesothelial to form a pro-metastatic microenvironment.

A) Western blot analysis evaluating the expression of the indicated proteins in whole cell lysates of mesothelial cells, OVSAHO and TOV-112D PT-sen and PT-res. Calretinin and Cytokeratin 5 were used as accepted marker of mesothelial cells and GAPDH as loading control. B) Western blot analysis evaluating the expression of the indicated proteins in whole cell lysates of mesothelial cells conditioned for the indicated times with CM of TOV-112D PT-res ITGA6KO cells in presence or not of an anti-IGFBP6 blocking antibody. Tubulin was used as loading control. C) Graph reporting the mRNA expression of IGF2 and LAMA5 (LM) genes in TOV-112D PT-sen cells challenged with conditioned medium (CM) of PT-res ITGA6 WT in presence or not of the specific anti-ITGA6 GoH3, or with CM of PT-res ITGA6 KO cells. D) Table reporting ITGA6 protein levels in ascitic fluids (measured by ELISA) and CA125 levels in blood samples (measured during clinical follow up) from 7 EOC patients. Samples from PT-res patients are in red. For 6 patients, two samples and for 1 patient, 4 samples, were collected at different times of clinical history. The clinical history of each patient is reported in the Methods section and in Figure 5F. E) Graph reporting the area of ovaryspheres formed by TOV-112D PT-sen cells plated on mesothelial cells monolayer challenged or not with ascites samples of EOC patient n.7 (see Methods) in the presence or not of the specific anti-ITGA6 blocking antibody, GoH3. F) Graph reporting the mRNA expression of IGF2 and LAMA5 (LM) in mesothelial cells incubated with ascites samples described in F in presence or not of the specific anti-ITGA6 blocking antibody, GoH3. In C and F, mRNA expression was analyzed in triplicate and normalized to actin. Statistical significance was determined by a two-tailed, unpaired Student's t-test (Exact *p* values were reported on graphs).

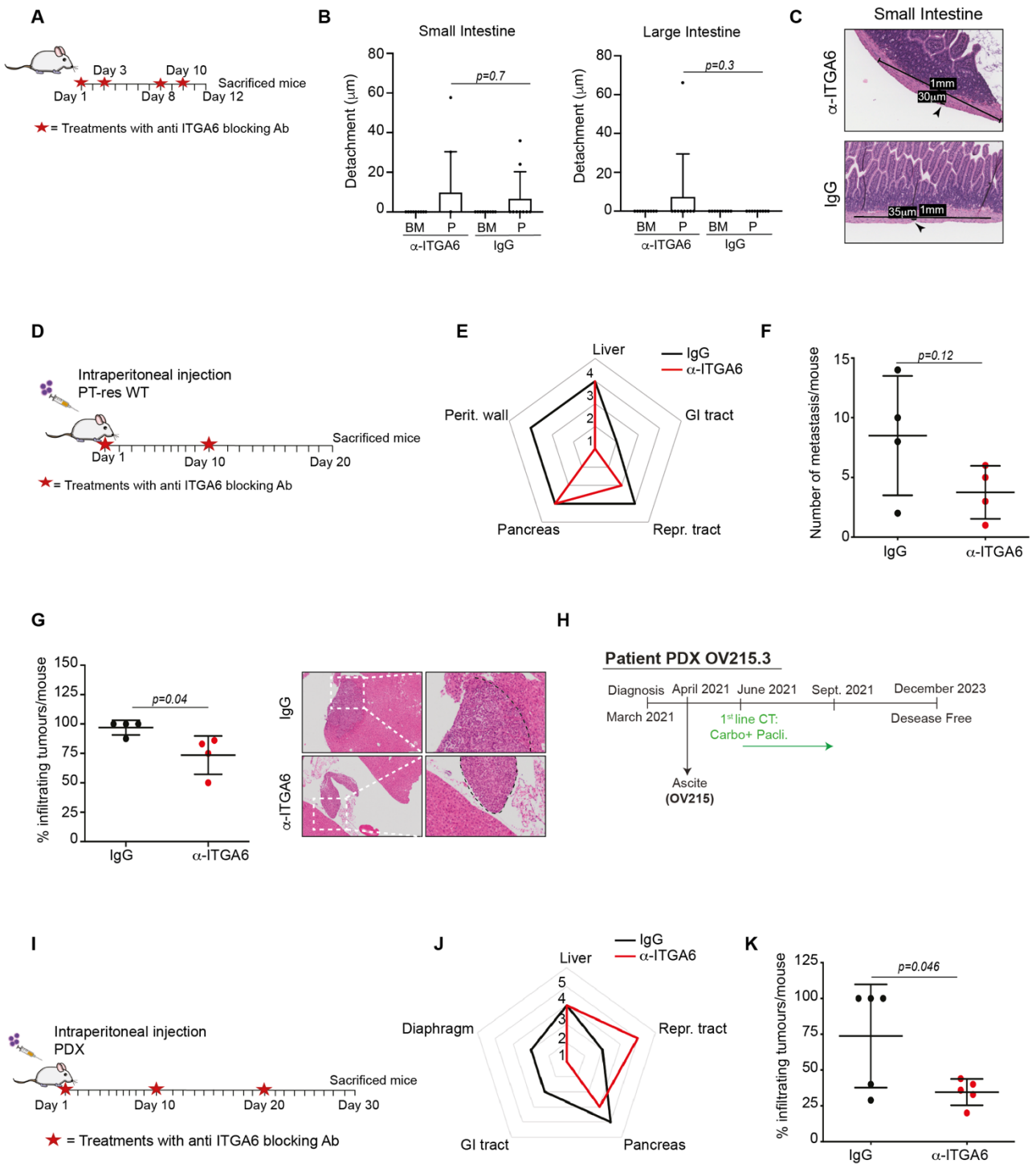

Appendix figure S5 (related to Figure 6).

A) Schematic representation of the *in vivo* experimental procedures used. C57BL6 mice were treated with the P5G10 specific anti-ITGA6 blocking antibody (n=3) or with IgG control antibody (n=3) according to the scheme. B-C) Graph (B) and typical H&E images (C) reporting the detachment from basement membrane (BM) or peritoneum (P) of epithelial cells of small and large intestine (see Methods) of mice reported in A. D) Schematic representation of the *in vivo* experimental procedures used. NSG mice injected intraperitoneally (IP) with PT-res ITGA6WT cells (n = 8), were randomly

divided into two group and treated or not with the P5G10 specific anti-ITGA6 blocking antibody, according to the scheme. E-F) Radar (E) and Dot (F) plots reporting the distribution of abdominal metastasis (E) and the total number of metastasis infiltrated in organs of abdomen (F) in mice injected intraperitoneally as in D, as determined by macroscopic and pathological analyses. In E, black and red lines indicate the number (values 0 to 4) of mice affected for each indicated district. J) Graph reporting the percentage of non-infiltrating tumors in mice described in D-F. On the right, typical images of H&E analyses of the liver from mice described in D-F. In P5G10 treated mice PT-res cells after did not infiltrate the liver. For each mouse, 5X and 10X images of the same field are shown. White dashed boxes represent the areas magnified in the right panels. H) Clinical history reporting the timeline of chemotherapy treatments (in green) and ascites collection of EOC patient who donate her ascites to establish PDX OV215.3 (see Methods section) I) Schematic representation of the *in vivo* experimental procedures using EOC PDX model. NSG mice injected IP with PDX OV215.3 (n =10), were randomly divided into two group and treated or not with the specific anti-ITGA6 blocking antibody, P5G according to the scheme. J) Radar plot reporting the distribution of abdominal metastasis in mice injected intraperitoneally as in I, as determined by macroscopic and pathological analyses. Black and red bold lines indicate the number (values 0 to 5) of mice affected for each indicated district. M) Graph reporting the percentage of infiltrating tumors in mice described in I-J. Statistical significance was determined by a two-tailed, unpaired Student's t-test (Exact *p* values were reported on graphs).

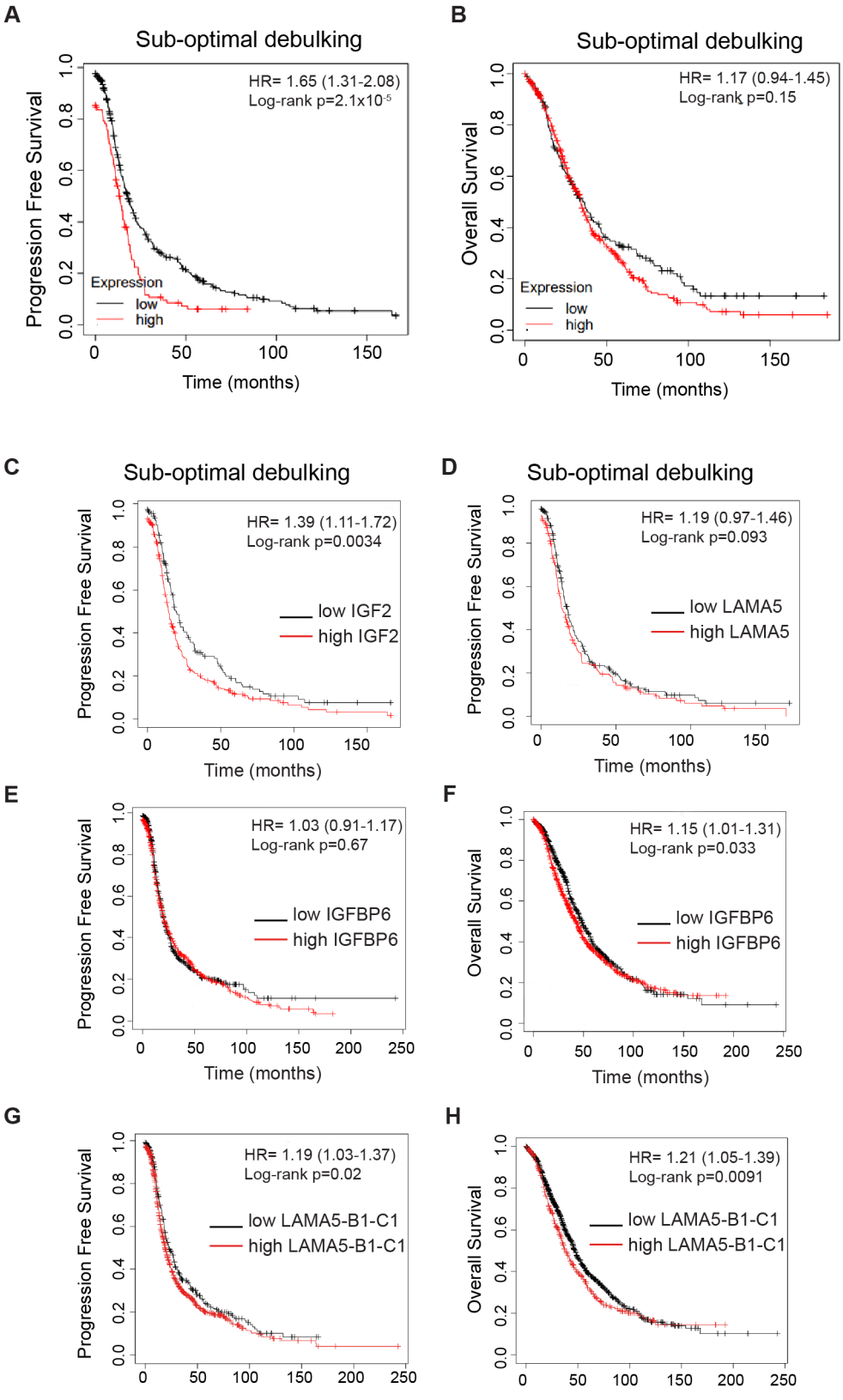

Appendix figure S6 (related to Figure 7). High ITGA6 expression and activity predict poor prognosis of EOC patients.

A-B) Kaplan Meyer estimating the progression free (PFS) (n=459) (A) or Overall survival (OS) (n=536) (B) of high risk suboptimal debulked advanced EOC patients, stratified for ITGA6 mRNA expression. C-D) Kaplan Meyer estimating the progression free survival (PFS) of patients described in A and B stratified for IGF2 (C) and LAMA5 (D) expression. E-F) Kaplan Meyer estimating the progression free (PFS) (n=1435) (E) or Overall survival (OS) (n=1656) (F) of EOC patients stratified for IGFBP6 expression. G-H) Kaplan Meyer estimating the progression free (PFS) (n=1435) (E) or Overall survival (OS) (n=1656) (F) of EOC patients stratified for the expression of LM10 components LAMA5B1 and C1 expression.

All Kaplan Meier curves were obtained using the KM Plotter dataset and on-line resource. HR = Hazard Ratio. The Confidence interval is reported between brackets. The p value was calculated using the logrank test.

Appendix Tables S1. Clinical-pathological features of ovarian cancer patients

Appendix Table S1A Clinical-pathological features of 27 ovarian cancer patients who donated their ascites samples (described in Figure 1C)

Characteristic	Distribution
Age-Year at diagnosis	
Median	66 y
Range	44-85 y
Histotype	
Serous	24 (88.9%)
Clear cell	1 (3.7%)
Mixed	1 (3.7%)
Not Available or Specified	1 (3.7%)
Tumor Stage	
I or II	0 (0%)
III or IV	25 (92.6%)
Not Available or Specified	2 (7.4%)
Samples Type	
Primary	16 (47%)
Recurrence	18 (53%)

Appendix Table S1B Clinical-pathological features of 30 ovarian cancer patients who donated their tumor samples (described in Figure 2I)

Characteristic	Distribution
Age-Year at diagnosis	
Median	67 y
Range	41-85 y
Histotype	
Serous	23 (76.7%)
Clear cell	1 (3.3%)
Mucinous	1 (3.3%)
Endometrioid	3 (10%)
Not Available or Specified	2 (6.7%)
Tumor Grade	
G1 or G2	3 (10%)
G3	16 (53.3%)
Not Available or Specified	11 (36.7%)
Samples Type	
Primary	23 (71.9%)
Recurrence	8 (25%)
Not Available or Specified	1 (3.1%)

Appendix Table S2. List of the 71 Human Receptor Tyrosine Kinases (RTKs) evaluated using a phospho-antibody array.

Protein	Position 1 in Array	Position 2 in Array	Protein	Position 1 in Array	Position 2 in Array
ABL1	G1	H1	IGF-I R	K7	L7
ACK1	I1	J1	Insulin R	A8	B8
ALK	K1	L1	Itk	C8	D8
Axl	E2	F2	JAK1	E8	F8
Blk	G2	H2	JAK2	G8	H8
BMX	I2	J2	JAK3	I8	J8
Btk	K2	L2	LCK	K8	L8
Csk	A3	B3	LTK	A9	B9
Dtk	C3	D3	Lyn	C9	D9
EGFR	E3	F3	MATK	E9	F9
EphA1	G3	H3	M-CSFR	G9	H9
EphA2	I3	J3	MUSK	I9	J9
EphA3	K3	L3	NGFR	K9	L9
EphA4	A4	B4	PDGFR-α	A10	B10
EphA5	C4	D4	PDGFR-β	C10	D10
EphA6	E4	F4	PYK2	E10	F10
EphA7	G4	H4	RET	G10	H10
EphA8	I4	J4	ROR1	I10	J10
EphB1	K4	L4	ROR2	K10	L10
EphB2	A5	B5	ROS	A11	B11
EphB3	C5	D5	RYK	C11	D11
EphB4	E5	F5	SCFR	E11	F11
EphB6	G5	H5	SRMS	G11	H11
ErbB2	I5	J5	SYK	I11	J11
ErbB3	K5	L5	Tec	K11	L11
ErbB4	A6	B6	Tie-1	A12	B12
FAK	C6	D6	Tie-2	C12	D12
FER	E6	F6	TNK1	E12	F12
FGFR1	G6	H6	TRKB	G12	H12
FGFR2	I6	J6	TXK	I12	J12
FGFR2 (α isoform)	K6	L6	Tyk2	A13	B13
Fgr	A7	B7	TYRO10	C13	D13
FRK	C7	D7	VEGFR2	E13	F13
Fyn	E7	F7	VEGFR3	G13	H13
Hck	G7	H7	ZAP70	I13	J13
HGFR	I7	J7			

Appendix Table S3. List of cytokines' expression evaluated using antibodies arrays.

Increased in ITGA6KO cells				Decreased in ITGA6KO cells		
Protein	**Mean fold KO/WT**	**p value**		**Protein**	**Mean fold KO/WT**	**p value**
IGFBP6	**7,60726273**	**0,00259226**		**IGFBP3**	**0,56620282**	**0,03501948**
IL-4	**3,98756299**	**0,03336018**		**ICAM-1**	**0,56868027**	**0,0256188**
ANGIOGENIN	**3,16054597**	**0,00013727**		**FLT3**	**0,59413795**	**0,01278056**
IGFBP2	**2,18686592**	**0,01001204**		**ICAM-3**	**0,62159453**	**0,03618497**
M-CSF	**1,27102446**	**0,01358263**		**ENA78**	**0,64296381**	**0,03724934**
MCP-2	1,72252928	0,05194512		**FGF**	**0,72552341**	**0,03069529**
MCP-4	1,40692253	0,06405499		**OPG**	**0,73821297**	**0,02964792**
SDF1 ALPHA	3,80355602	0,07085209		**TPO**	-0,1998336	0,0812738
MDC	1,23726839	0,10236117		**DTK**	0,4625478	0,0991287
IL-2	4,29305922	0,10908557		**U PAR**	0,73230461	0,11029694
MIP-1 DELTA	1,22047082	0,12563879		**GRO**	0,5393833	0,1142779
RANTES	1,27908259	0,16169678		**GP130**	0,68936283	0,11514977
CKB	1,14842809	0,1714551		**IL17A**	0,58166966	0,12654988
MIP-3 ALPGA	1,11217802	0,18449984		**NT4**	0,78921162	0,1288513
CNTF	1,15477668	0,18867736		**IL2-R ALPHA**	0,53494674	0,14121554
FCS	1,20743884	0,20190817		**BTC**	0,52073699	0,15689012
IL-1 RA	1,14972407	0,21368617		**HCC4**	0,67579161	0,16380249
TARC	10,1232911	0,23359752		**PLGF**	0,73456174	0,1714423
IL-1 BETA	1,24636819	0,28056495		**EGFR**	0,72194056	0,17730985
MCP-3	1,54361467	0,29283559		**TNFR II**	0,74950935	0,19082892
TNFALPHA	1,10609835	0,30273207		**TRAIL R3**	0,59666908	0,197282
EOTAXIN 2	2,18578346	0,3031799		**IL10**	-0,8809363	0,20539987
FRACTALKINE	1,83099072	0,31259744		**MFP**	0,86170364	0,20605745
I 309	1,2077951	0,37323091		**FGF7**	0,50280522	0,21779143
TGFB-1	1,41431516	0,37446202		**BMP6**	0,89250222	0,25100403
IL12P70	2,88069532	0,38658551		**IL1R1**	0,6543451	0,28432238
BDNF	1,14816513	0,42265431		**FAS**	0,55007343	0,28572522
IL-15	1,10151066	0,46008126		**IL12**	0,6095377	0,31237351
MIP1-ALPHA	1,56427029	0,52446394		**GM-CF**	0,64930287	0,31241002
TRAILR4	1,14515052	0,53179388		**MIP3 BETA**	0,9547971	0,33374571
FGF6	1,39291529	0,55591669		**TNFR I**	0,88729022	0,33922719
EOTAXIN 1	1,14568747	0,58720008		**LINFO-TACTIN**	0,71673848	0,33968487
IGFBP4	1,12148666	0,58865929		**ANGPT2**	0,73880407	0,35520446
GITR LIGAND	1,30601349	0,59351996		**BLC**	0,88543844	0,37097138
VEGFA	1,23696918	0,59520312		**IL-6**	0,98026317	0,38256769
IL-5	1,67547386	0,64292036		**NAP 2**	0,90334025	0,40022551
PARC	1,24882403	0,65785083		**IL11**	-12,554783	0,42385339

LIGHT	1,22192523	0,67209221		**IL8**	0,7202121	0,43157637
MCP-1	1,18219289	0,76801011		**AGRP**	0,90287898	0,43746076
IL-1 ALPHA	4,41377465	0,76887339		**FGF-9**	0,61715803	0,43919227
MIF	1,36625048	0,77971979		**GRO ALPHA**	0,87244127	0,4671164
MIP1 BETA	1,45903189	0,78277198		**HGF**	0,81689038	0,47975854
OSM	1,00771943	0,80637878		**IL1-R4**	0,76757434	0,51505746
TGFB-3	1,02253113	0,81933787		**TIMP-2**	-2,3621273	0,52452802
I-TAC	1,05211575	0,82963791		**IGF1**	0,09618227	0,55393744
ADIPONECTIN	1,01142549	0,82991505		**CTACK**	0,74240727	0,55447907
TIMP-1	1,19550401	0,86846005		**NT3**	0,92014971	0,56044665
EGF	1,08276751	0,87252863		**EOTXIN**	0,64385716	0,56760307
GITR	1,02950406	0,8879063		**AXL**	0,88849374	0,6045616
IGFBP1	1,01018224	0,89149755		**BETA -NGF**	0,98074688	0,63137257
IF-GAMMA	1,03158786	0,90612767		**TECK**	0,62953616	0,66818978
BMP4	1,05890457	0,90908748		**IL-13**	0,19468073	0,71956117
FGF-4	1,09451424	0,90964464		**IL6-R**	0,72397634	0,73688025
AR	1,05791526	0,91340046		**IL-7**	0,87120922	0,80539469
G-CSF	1,18503923	0,91911604		**VEGFD**	-6,5090324	0,86187842
IL-16	1,14248323	0,92081228		**TNF BETA**	0,97656925	0,99057864
MIG	1,04268888	0,92688154				
LEPTIN	1,03285899	0,92703065				
PDGF BB	1,00911221	0,93587066				
GCP2	1,00697823	0,93748127				
GDNF	1,02211736	0,95240945				
IGF1R	1,0676378	0,95495183				
IL-3	1,02049936	0,98978723				

List of cytokines evaluated in the conditioned medium of ITGA6WT and ITGA6KO TOV112D PT-Res cells.
Data are expressed as the mean ratio of each cytokine levels in the medium of ITGA6KO on its levels in the medium of ITGA6WT cells. The significance ($p<0.05$) of the difference among samples was evaluated by unpaired t-test. Data are the mean of 2 biological replicates each performed in duplicate using an antibody cytokine array (Human Cytokine Array C6-C8 from RayBiotech).

Appendix Table S4. List and dilutions of Antibodies used.

Antibody	Dilution	Sources	Catalog number/identifier
c-Myc	WB 1:1000	Cell Signaling Technology	5605; RRID/AB_1903938
c-Myc	WB 1:200	Santa Cruz Biotechnology	sc-40; RRID/AB_627268
Snail	WB 1:1000	Cell Signaling Technology	3879; RRID/AB_2255011
Snail/Slug	IF 1/50	Abcam	ab180714; RRID/AB_2728773
Slug	WB 1:1000	Cell Signaling Technology	9585; RRID/AB_2239535
Phospho p44/42 MAP kinase (T202/Y203)	WB 1:1000	Cell Signaling Technology	9101; RRID/AB_331646
ERK1	WB 1:300	Santa Cruz Biotechnology	sc-271269; RRID/AB_10611091
Phospho-Akt (S473)	WB 1:2000	Cell Signaling Technology	9271; RRID/AB_329825
Akt	WB 1:500	Cell Signaling Technology	9272; RRID/AB_329827
Phospho-Lyn (Y507)	WB 1:1000	Cell Signaling Technology	2731; RRID/AB_2138262
Phospho Lyn (Y397)	WB 1:1000	Abcam	ab226778; RRID/AB_2928952
Lyn	WB 1:1000	Cell Signaling Technology	2796; RRID/AB_2138391
TCF8/ZEB1	WB 1:1000	Cell Signaling Technology	3396; RRID/AB_1904164
Phospho-IGF-I Receptor beta (Y1135)	IF 1/50; WB 1:1000	Cell Signaling Technology	3918; RRID/AB_10548764
IGF-I Receptor beta	WB 1:500	Cell Signaling Technology	9750; RRID/AB_10950969
Phospho-mTOR (S2448)	WB 1:1000	Cell Signaling Technology	2971; RRID/AB_330970
mTOR	WB 1:500	Cell Signaling Technology	2983; RRID/AB_2105622
Phospho-Src Family (Y416)	WB 1:500	Cell Signaling Technology	2101; RRID/ AB_331697
c-Src	WB 1:500	Santa Cruz Biotechnology	sc-5266; RRID/AB_627308
4E-BP1	WB 1:1000	Cell Signaling Technology	9644; RRID/AB_2097841
Anti-4E-BP1, phospho (T37/T46)	WB 1:1000	Cell Signaling Technology	2855; RRID/AB_560835
Vinculin	WB 1:500	Santa Cruz Biotechnology	sc-7649; RRID/AB_2288413
alpha Tubulin	WB 1:500	Santa Cruz Biotechnology	sc-32293; RRID/AB_628412
Twist	WB 1:200	Santa Cruz Biotechnology	sc-81417; RRID/AB_1130910
ITGA6	WB 1:1000	Merk-Sigma	APREST78051; RRID/AB_2928950
ITGA6	WB 1:1000	Cell Signaling Technology	3750; RRID/AB_2249263
SP1	WB 1:500	Merk-Sigma	SAB1404397; RRID/AB_10759217
HDAC1	WB 1:1000	Merk-Sigma	H3284; RRID/AB_260039
GAPDH	WB 1:1000	Millipore	CB1001, RRID/AB_2107426
IRS1	WB 1:1000	Millipore	05-1085; RRID/AB_1977296
IGF-II	WB 1:1000	R&D	792-MG; RRID/AB_2928954

IGFBP6	In vitro 10 µg/ml WB 1:500	R&D	AF876; RRID/AB_355679
Phospho-FAK (Y397)	WB 1:1000	Thermo Fisher Scientific	44-624G, RRID/AB_2533701
FAK	WB 1:1000	BD Biosciences	610087, RRID/AB_397494
PE Anti-CD49a	FACS 10ml/1x10^{6}cells	BD Biosciences	559596, RRID/AB_397288
PE Anti-CD49b	FACS 10ml/1x10^{6}cells	BD Biosciences	553858, RRID/AB_395094
APC Anti-CD49d	FACS 10ml/1x10^{6}cells	BD Biosciences	561892, RRID/AB_10896134
PE Anti-CD49e	FACS 10ml/1x10^{6}cells	BD Biosciences	555617, RRID/AB_395984
PE Anti-CD49f	FACS 10ml/1x10^{6}cells	BD Biosciences	555736, RRID/AB_396079
PE Anti-CD51	FACS 10ml/1x10^{6}cells	BD Biosciences	551187, RRID/AB_394088
PE Anti-CD29	FACS 10ml/1x10^{6}cells	BD Biosciences	557332, RRID/AB_396646
PE Anti-CD61	FACS 10ml/1x10^{6}cells	BD Biosciences	555754, RRID/AB_396095
PE Anti-CD104	FACS 10ml/1x10^{6}cells	BD Biosciences	555720, RRID/AB_396063
Goat anti-Mouse IgG2b Antibody HRP-Conj.	WB 1:5000	Bethyl	A90-109P, RRID/AB_67160
Goat anti-Rabbit IgA Antibody HRP-Conj.	WB 1:5000	Bethyl	A120-109P, RRID/AB_67251
Purified anti-human/ mouse CD49f (GoH3)	In vitro 10 µg/ml;	BioLegend	313602, RRID/AB_345296
Purified Rat IgG2a, κ Isotype Ctrl Antibody	FACS 10ml/1x10^{6}cells	BioLegend	400501, RRID/AB_326523
Integrin alpha-6, human blocking Ab (P5G10)	In Vivo 30mg/kg IF 3mg/ml	DSHB	P5G10, RRID/AB_2619593
Alexa Fluor™ 647 Phalloidin	IF 1:200	Invitrogen	A22287
TO-PRO-3 Iodide (642/661)	IF 1:500	Invitrogen	T3605
IRDye® 680RD Goat anti-Mouse IgG Sec. Ab	WB 1:1500	LI-COR	926–68070, RRID/ AB_10956588
IRDye® 680RD Goat anti-Rabbit IgG Sec. Ab	WB 1:1500	LI-COR	926–68071; RRID/ AB_10956166
IRDye® 800CW Goat anti-Mouse IgG Sec. Ab	WB 1:1500	LI-COR	926–32210; RRID/ AB_621842
IRDye® 800CW Goat anti-Rabbit IgG Sec. Ab	WB 1:1500	LI-COR	926–32211; RRID/ AB_621843

Appendix Table S5. List of Oligonucleotides used for RT-PCR and ChIP analysis

Oligo Name	Sequence
ITGA6 promoter (FL) FW	*CTCGAG*TTTTGAGGGTTGTTAGG
ITGA6 promoter Rev	*AGATCT*GGGTCGCGCTCTCCGTCCGG
ITGA6 promoter (MUT1) FW	*CTCGAG*GGCCACATCTGCAAG
gITGA6-3 FW	GGGCTGCAGTTGCCAGTGCA
gITGA6-3 Rev	TGCACTGGCAACTGCAGCCC
gITGA6-6 FW	AGAAGCCGAAGAGGCTCCCG
gITGA6-6 Rev	CGGGAGCCTCTTCGGCTTCT
ITGA6 for ChIP FW	TTGTGTACATTATACAGCAC
ITGA6 for ChIP Rev	GGAGACTTTACTACCCGTTATAAA
ITGA6 for qRT-PCR FW	AAGTCTCGTTCCTGTTCCTGC
ITGA6 for qRT-PCR Rev	ACTGTGATTGGCTCTGGGAG
ITGA6A for qRT-PCR FW	GAGATCCATGCTCAGCCATC
ITGA6A for qRT-PCR Rev	ACTGTCATCGTACCTAGAGCGTTT
ITGA6B for qRT-PCR FW	ACTATGGAAGTGTGGATTCTTT
ITGA6B for qRT-PCR Rev	CCCCCGCTATGAGTAGCTTT
Actin for qRT-PCR FW	CCAGAGGCGTACAGGGATAG
Actin for qRT-PCR Rev	CCAACCGCGAGAAGATGA
SP1 for qRT-PCR FW	GGTGCCTTTTCACAGGCTC
SP1 for qRT-PCR Rev	CATTGGGTGACTCAATTCTGCT
MYC for qRT-PCR FW	CTCCTGGCAAAAGGTCAGAG
MYC for qRT-PCR Rev	TCGGTTGTTGCTGATCTGTC
LAMA5 for qRT-PCR FW	GACTGCCAACAGTGCCAAC
LAMA5 for qRT-PCR Rev	CCACCCTGATAGGTGCCAT
IGF-II for qRT-PCR FW	GAAGATGCTGCTGTGCTTCC
IGF-II for qRT-PCR Rev	AGTGAGCAAAACTGCCGC
IGFBP6 for qRT-PCR FW	AATCCAGGCACCTCTACCA
IGFBP6 for qRT-PCR Rev	GCCCATCCGATCCACA